Available online at www.sciencedirect.com
ScienceDirect
Journal of Luminescence 128 (2008) 341–347
JOURNAL OF LUMINESCENCE
www.elsevier.com/locate/jlumin

Optical oxygen sensing materials based on trinuclear starburst ruthenium(II) complexes assembled in mesoporous silica

Binbin Wang[a,b], Yana Liu[c], Bin Li[a,*], Shumei Yue[a], Wenlian Li[a]

[a]*Key Laboratory of Excited State Processes, Changchun Institute of Optics Fine Mechanics and Physics, Chinese Academy of Sciences, Changchun 130033, PR China*
[b]*Polyoxometalate Science Key Laboratory of Ministry of Education, Department of Chemistry, Northeast Normal University, Changchun 130024, PR China*
[c]*Key Laboratory of Tropical Marine Environmental Dynamics, South China Institute of Oceanology, Chinese Academy of Sciences, Guangzhou 510301, PR China*

Received 25 December 2006; received in revised form 24 August 2007; accepted 28 August 2007
Available online 26 November 2007

Abstract

The preparation and oxygen sensing properties of optical materials based on two trinuclear starburst ruthenium(II) complexes: $[Ru_3(bpy)_6(TMMB)]^{6+}$ (**1**) and $[Ru_3(phen)_6(TMMB)]^{6+}$ (**2**) (bpy = 2,2′-bpyridine, phen = 1,10-phenathroline, TMMB = 1,3,5-tris [2-(2′-pyridyl)benzimidazoyl]methylbenzene) assembled in two mesoporous silicate (MS) are described in this paper. The luminescence of Ru complexes/silicate assemble materials can be quenched by molecular oxygen with good sensitivity ($I_0/I_1 > 5$ for **2**/MS and $I_0/I_1 > 3$ for **1**/MS), indicating that trinuclear starburst Ru(II) complexes/MS systems are sensitive to oxygen molecules.

Keywords: Oxygen sensor; Trinuclear starburst Ru(II) complexes; Mesoporous silicate

1. Introduction

In the past decades, luminescence-based optical oxygen sensors have been greatly developed in medicinal, environmental, and analytical chemistry [1–6]. They are the most widely used in wonderful performances such as faster response time, high sensitivity and selectivity, no O_2 consumption, no poison and no requirement for a reference electrode, long-term stability, and good non-linear calibration plots [7–16]. For optical oxygen sensors, an important method is based on the luminescence quenching of luminophore by the presence of oxygen, which is based on the principle that oxygen is a powerful quencher of the electronically excited state of luminescence dyes molecule. The excited-state lifetime and emission intensity of the luminophore decrease as the oxygen concentration increases. Many luminescent dyes have been developed as oxygen sensing materials. Among them, luminescent transition metal complexes, particularly those of Ru(II) polypyridyl compounds, have been frequently utilized [15,17,18], due to highly emissive metal-to-ligand charge-transfer (MLCT) state, long fluorescence lifetime, large Stokes shift, high photochemical stability, high sensitivity to oxygen and strong ultraviolet visible absorption in the blue–green region of the spectrum [12,13,15,19], and the host materials such as sol–gel and polymer films are used to encapsulate the luminescent complexes.

In recent years, immobilizing the functional molecules into ordered mesoporous molecular sieves has received considerable attention [20–23]. Since the development proved by the Mobil Oil Company of the class of periodic mesoporous silicas known as M41S in 1992, ordered mesoporous materials with unique properties of high surface area, ordered pore structure of varying morphologies, and controllable pore size over wide ranges which have been widely investigated with regard to their potential applications as catalysts, adsorbents for large organic molecules, chromatography and sensor technology. Mesoporous materials are able to physically encapsulate and immobilize the functional molecules into the pores, while the solvent and other small molecules or ions are allowed

*Corresponding author. Tel.: +86 431 6176935; fax: +86 431 6176935.
E-mail address: lib020@ciomp.ac.cn (B. Li).

0022-2313/$ - see front matter © 2007 Elsevier B.V. All rights reserved.
doi:10.1016/j.jlumin.2007.08.011

into the interior of the mesoporous silicas through channels. Starburst transition metal complexes which possess excellent luminescence properties because their special structure could efficiently avoid the triplet–triplet annihilation [24]. However, supporting our knowledge, there are no reports on the usage of starburst metal complexes as luminescence-based optical oxygen sensors. In this paper, we first present the preparation and properties of four oxygen sensing materials based on two trinuclear starburst Ru(II) complexes: **1**/SBA-15, **1**/MCM-41, **2**/SBA-15, and **2**/MCM-41. The results indicate starburst Ru(II) complexes are sensitive to oxygen molecules.

2. Experimental

The synthesis route of trinuclear starburst Ru(II) complexes is depicted in Scheme 1.

2.1. Synthesis and characterization of 1,3,5-tris (bromomethyl) benzene (*4*)

A mixture of mesitylene (**5**) (2.8 ml, 0.02 mol), *N*-bromosuccinimide (NBS) (10.62 g, 0.06 mol), and benzoyl peroxide (BPO) (0.11 g) in CCl_4 (30 ml) is stirred and heated under N_2 for 14 h at 90 °C. After filtering, the filtrate is washed by water and dried by anhydrous $MgSO_4$. Upon concentration of the CCl_4 solution, a colorless needle crystal is precipitated. Recrystallization in a 1:1 mixture of ethanol/hexane affords 6.56 g product (yield, 92%). ^{1}H NMR (CD_3OD): δ 4.55 (s, 6 H), 7.42 (s, 3 H).

2.2. Synthesis and characterization of TMMB (*3*)

A mixture of 1,3,5-tris(bromomethyl) benzene (0.357 g, 1 mmol), PyBM (0.600 g, 3 mmol), sodium hydroxide (0.12 g, 3 mmol), and DMF (30 ml) is stirred and heated under N_2 for 15 h at 120 °C. It is subsequently poured into ice water (100 ml), after extraction with dichloromethane (3 × 30 ml). The organic layer is washed by water and dried over anhydrous $MgSO_4$. The solvent is then evaporated, the resulted residue is purified by silica gel column chromatography to give 0.11 g product. ^{1}H NMR (500 MHz, $CDCl_3$): δ 5.89 (s, 6H), 6.90 (s, 3H), 7.05–7.08 (t, 3H), 7.14–7.19 (t, 6H), 7.28–7.32 (d, 3H), 7.69–7.73 (t, 3H), 7.83–7.85 (d, 3H), 8.19–8.26 (d, 6H). EI-mesoporous silicate (MS): *m*/*z*: 700 (M^+).

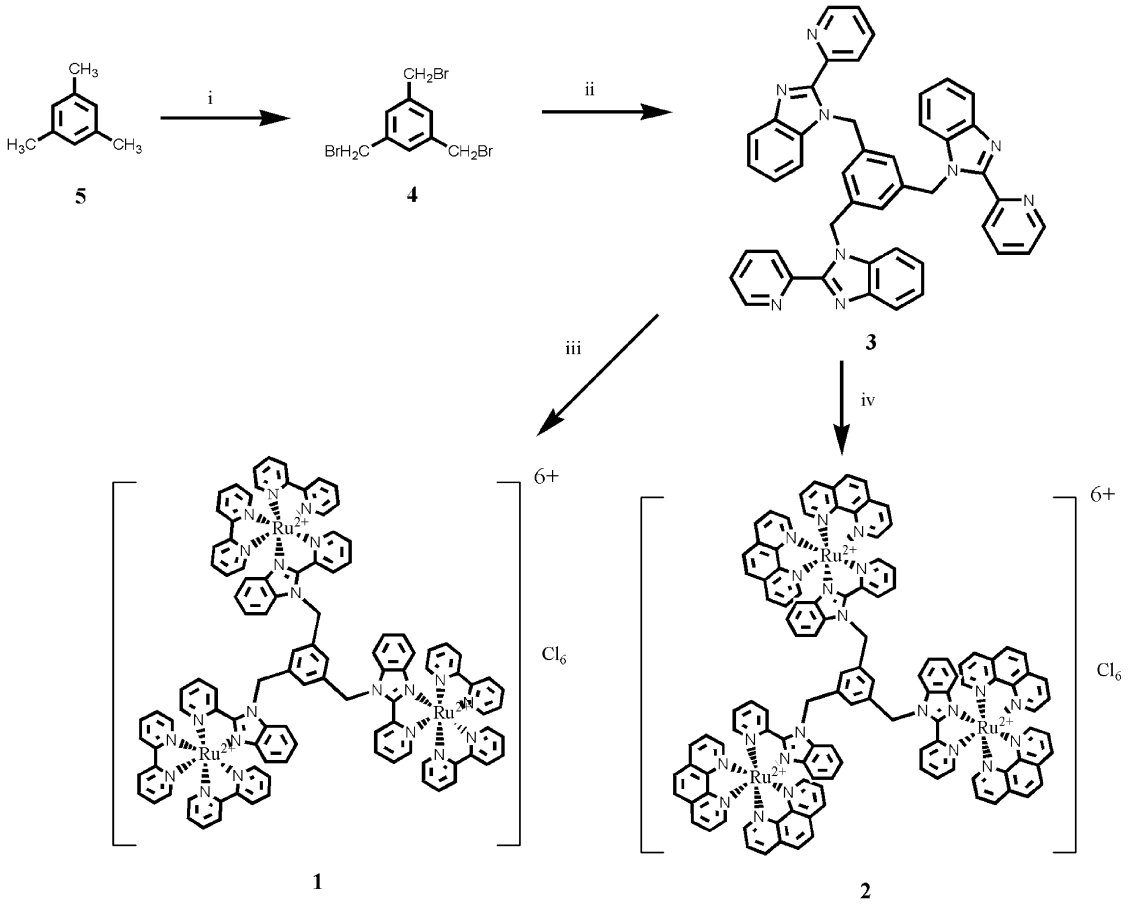

Scheme 1. Synthetic route to **1** and **2**. *Reagents*: (i) *N*-bromosuccinimide, CCl_4, 90 °C, 14 h; (ii) 2-(2-pyridyl)benzimidazole, DMF, 120 °C, 15 h; (iii) $Ru(bpy)_2Cl_2 \cdot 2H_2O$, ethanol, 80 °C, 4 h; and (iv) $Ru(phen)_2Cl_2 \cdot 2H_2O$, ethanol, 80 °C, 4 h.

2.3. Synthesis and characterization of (*1*) and (*2*)

$Ru(bpy)_2Cl_2 \cdot 2H_2O$ and $Ru(phen)_2Cl_2 \cdot 2H_2O$ are synthesized according to the published procedure [25,26]. A solution of $Ru(bpy)_2Cl_2 \cdot 2H_2O$ (0.22 g, 0.3 mmol) or $Ru(phen)_2Cl_2 \cdot 2H_2O$ (0.23 g, 0.3 mmol) and TMMB (0.07 g, 0.105 mmol) in ethanol (30 ml) is stirred and heated under N_2 for 4 h at 80 °C until the reactive solution changed into dark red. Upon concentration of the ethanol solution to 10%, diluted with water, boiled for 10 min, cooled in an ice-bath, and filtered. The filtrate is rotated and recrystallized from ether and dichloromethane. **1**: ^{1}H NMR (500 MHz, DMSO-d_6): δ 5.89 (s, 6H), 6.90 (s, 3H), 7.05–7.08 (t, 3H), 7.12–7.13 (t, 12H), 7.14–7.19 (t, 6H), 7.28–7.32 (d, 3H), 7.66–7.68 (d, 12H), 7.69–7.73 (t, 3H), 7.83–7.85 (d, 3H), 8.19–8.26 (d, 6H), 8.49–8.53 (d, 12H) 8.61–8.67 (d, 12H). Anal. Calcd for $C_{105}H_{81}Cl_6N_{21}Ru_3$. Calcd: C, 58.39; H, 3.88; N, 13.52. Found: C, 58.58; H, 3.77; N, 13.67; **2**: ^{1}H NMR (500 MHz, DMSO-d_6): δ 5.89 (s, 6H), 6.90 (s, 3H), 7.05–7.08 (t, 3H), 7.14–7.19 (t, 6H), 7.20–7.29 (t, 12H), 7.28–7.32 (d, 3H), 7.62–6.63 (d, 12H), 7.69–7.73 (t, 3H), 7.83–7.85 (d, 3H), 8.08–8.14 (d, 12H), 8.19–8.26 (d, 6H), 8.90–8.98 (d, 12H). Anal. Calcd for $C_{117}H_{81}Cl_6N_{21}Ru_3$. Calcd: C, 61.05; H, 3.49; N, 12.96. Found: C, 61.18; H, 3.53; N, 12.81.

The host materials MCM-41 [27] and SBA-15 [28] are prepared as described in the above literatures. The template is removed from the mesoporous silica by calcination according to the previous reports [27,28].

The luminophore Ru(II) complexes are incorporated into mesoporous molecular sieves to obtain the assembled materials as the following procedures described: 50 mg of the mesoporous host is added into the chloroform solution of ruthenium (II) complexes (1 mg), and the mixture is stirred under ambient conditions for 24 h. The resulted suspension is filtered which gives a yellow powder. Washing it repeatedly with chloroform until the filtered chloroform solution is colorless under UV illumination, the residual products are dried in air and the encapsulated Ru (II) complexes/MS (20 mg/g) are obtained as a yellow powder.

Powder X-ray diffraction (XRD) spectra are recorded on a Siemens D5005 diffractometer. UV–vis absorption spectra are obtained using a Cary 500 Scan UV–vis–NIR Spectrophotometer. Luminescence spectra and response curves are obtained using a Hitachi F-4500 fluorescence spectrophotometer. The pure oxygen and pure nitrogen are mixed together with different concentrations from which we can get the mixed gases for measurement.

3. Results and discussion

Powder XRD spectra of MCM-41, MCM-41-based systems, SBA-15 and SBA-15-based systems are shown in Fig. 1. It shows three Bragg reflections in the low angle indexed to d100, d110, and d200, which are characteristic peaks of highly ordered hexagonal (P6mm) mesostructure [29,30]. Powder XRD measurement results indicate that the hexagonal arrangement of channels in mesoporous molecular sieves remains unchanged after the incorporation of Ru(II) complexes.

UV–vis absorption spectra of **2**/MS are similar to that of **2** in chloroform (Fig. 2), indicating that the luminophors incorporated in composite systems remain intact and keep their photochemical properties unchanged during the process of encapsulation. The absorption band at 200–350 nm is tentatively ascribed to a $\pi \rightarrow \pi^*$ transition of ligand, and the absorption band at 455 nm is assigned to the [$d\pi(Ru) \rightarrow \pi^*$(ligand)] MLCT transition. By comparing the UV–vis absorption spectra of **1**/MS (20 mg/g) and **1** in chloroform, similar results were observed.

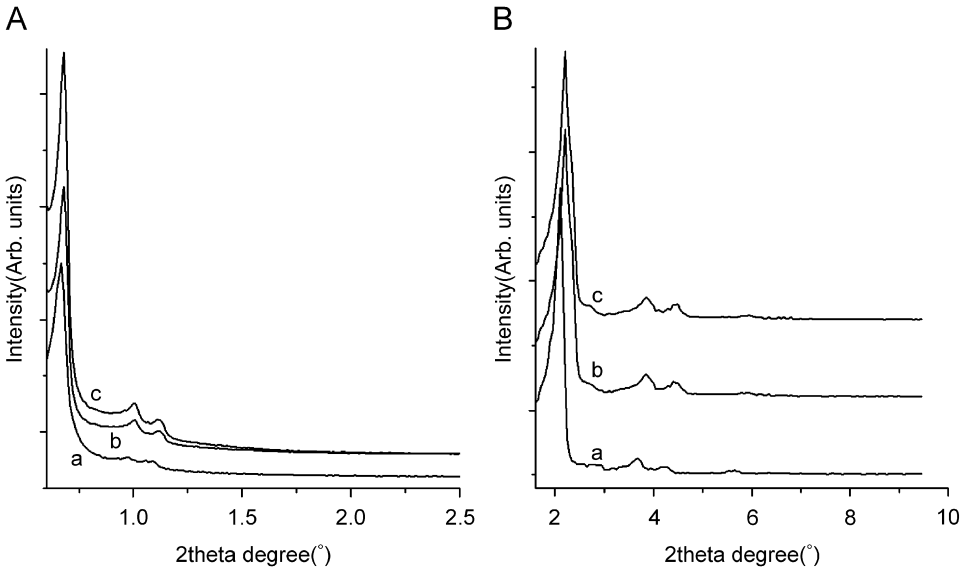

Fig. 1. (A) XRD patterns of SBA-15 (a), **1**/SBA-15 (b), and **2**/SBA-15 (c). (B) XRD patterns of MCM-41 (a), **1**/MCM-41 (b), and **2**/MCM-41 (c).

Emission quantum yield is defined as the ratio of the number of photons emitted to the number of photons absorbed. The luminescence quantum yields of the **1** and **2** in degassed CH_2Cl_2 have been confirmed by comparing with the known luminescence yield from $[Ru(bpy)_3Cl_2]\cdot 6H_2O$ in CH_3CN ($\Phi_r = 0.062$) [29]. Sample and standard solutions were degassed with no less than four freeze-pump-thaw cycles. Quantum yield is identified according to Eq. (1):

$$\Phi_s = \Phi_r \left(\frac{B_r}{B_s}\right)\left(\frac{n_s}{n_r}\right)^2\left(\frac{D_s}{D_r}\right) \quad (1)$$

where the subscripts s and r refer to sample and reference standard solution, respectively, n is refractive index of the solvent, D is the integrated intensity, and Φ is luminescence quantum yield. The quantity B is calculated by $B = 1\text{–}10^{-AL}$, where A is the absorbance at the excitation wavelength and L is the optical path length. The luminescence quantum yields of **1** and **2** in solution are 0.050 and 0.042 at a concentration of 1×10^{-5} M. These results indicate that trinuclear starburst Ru(II) complexes possess good luminescence properties in anaerobic surroundings.

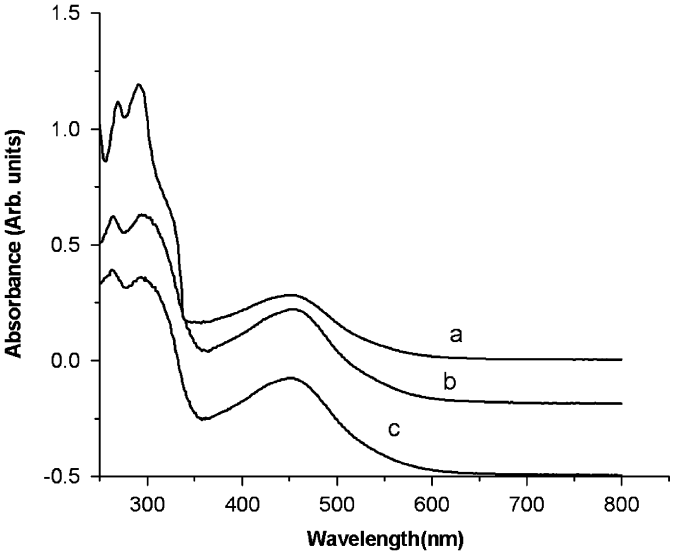

Fig. 2. UV–vis absorption spectra of **2** in chloroform (a), **2**/SBA-15 (b), and **2**/MCM-41 (c).

The luminescence of most Ru(II) complexes could be quenched effectively by molecular oxygen. The room temperature emissive spectra, which are recorded for **1**/SBA-15 (20 mg/g) and **2**/SBA-15 (20 mg/g) under different concentrations of oxygen, are presented in Fig. 3. The emission bands of **1**/SBA-15 (20 mg/g) and **2**/SBA-15 (20 mg/g) centered on 613 and 604 nm, respectively, and the relative intensity decreased markedly with increasing oxygen concentration. The luminescent intensities of **1**/SBA-15 and **2**/SBA-15 decrease by 69.7% and 81.0%, respectively, upon changing from pure nitrogen to pure oxygen conditions. The **2**/SBA-15 system is more sensitive compared with the **1**/SBA-15 system. Similar results are observed by comparing the emission spectra for **1**/MCM-41 and **2**/MCM-41 under different concentrations of oxygen.

Luminescent molecule quenching in homogeneous media with negligible matrix effects are expected showing single-exponential excited state decay, and the emission intensity or decay time with oxygen concentration can be described by the Stern–Volmer (SV) equation:

$$\frac{I_0}{I} = \frac{\tau_0}{\tau} = 1 + K_{SV}[Q] = 1 + K_{q\tau_0}[Q] \quad (2)$$

where I and τ are the luminescence intensity and the excited-state lifetime of the related decay profile, respectively, the subscript 0 denotes the absence of oxygen, K_{SV} is the Stern–Volmer constant, K_q is the bimolecular rate constant describing the efficiency of the collisional encounters between the luminophore and the quencher, and

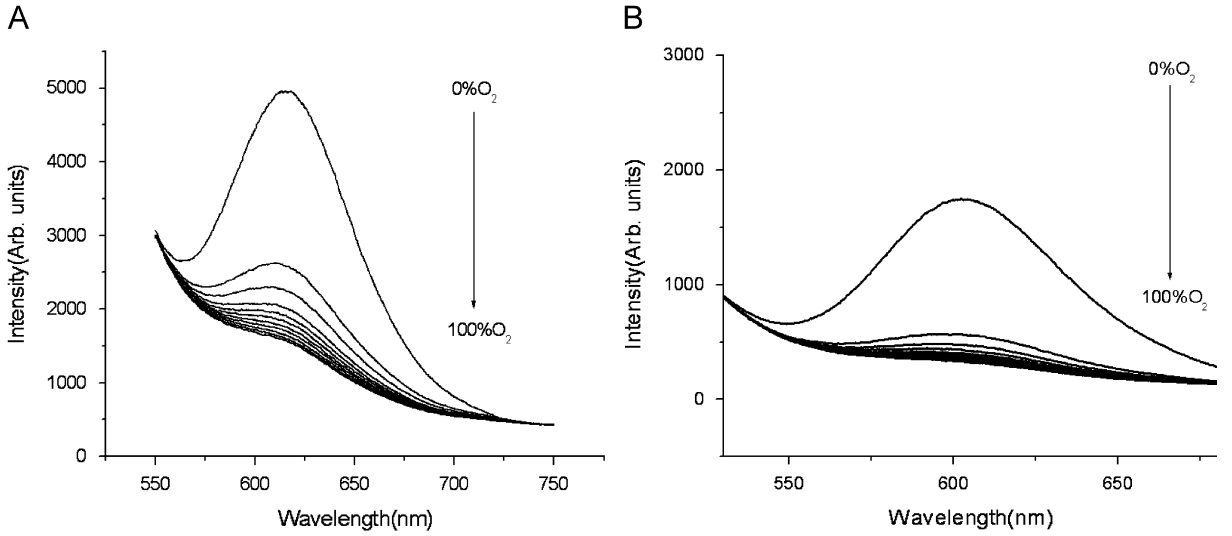

Fig. 3. Photoluminescence spectrum of **1**/SBA-15 (20 mg/g, (A)) and **2**/SBA-15 (20 mg/g, (B)) under different oxygen concentrations.

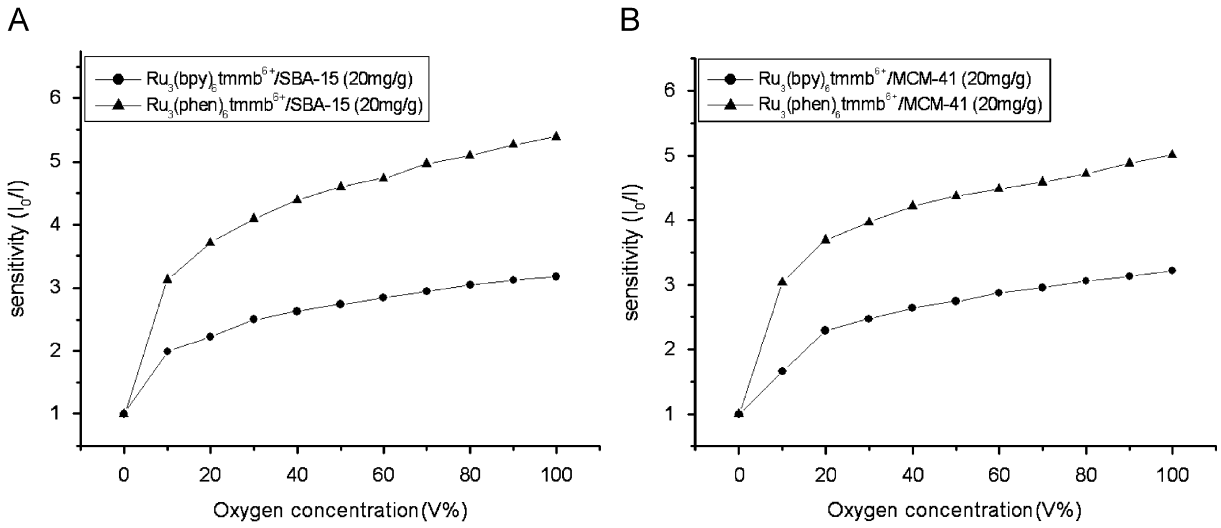

Fig. 4. Typical fluorescence intensity-based Stern–Volmer plots for (A) **1**/SBA-15 (20 mg/g) and **2**/SBA-15 (20 mg/g), (B) **1**/MCM-41(20 mg/g) and **1**/MCM-41 (20 mg/g).

[Q] is the O_2 concentration. In the ideal case, the plot of I_0/I or τ_0/τ versus oxygen concentration should give a straight-line relationship with slope K_{SV}. However, non-linear Stern–Volmer plots are often obtained when quenching takes place in a solid matrix [31–33]. Fig. 4 presents the Stern–Volmer plots for composite materials, respectively. The plots are non-linear within a wide range of oxygen concentrations. The deviation from linearity is attributed to a distribution of slightly different quenching environments for Ru(II) complexes. It is believed that there are two sites of starburst Ru(II) complexes' micro-environments within the mesoporous molecular sieves: one site is oxygen-easy accessible and the other is oxygen-difficult accessible. The luminophore molecules can be distributed simultaneously between two sites within the mesoporous materials in which one site is more heavily quenched than the other [34–37]. Starburst Ru(II) complexes may exhibit characteristic quenching constants within each distinct starburst Ru(II) complexes site, and the overall Stern–Volmer expression[33] becomes:

$$\frac{I_0}{I} = \frac{1}{(f_{01}/(1 + K_{SV1}[Q])) + (f_{02}/(1 + K_{SV2}[Q]))} \quad (3)$$

Here, I_0/I denotes the sensitivity, f_{01} and f_{02} denote the fractional contributions of the total intensity from the starburst Ru(II) complexes which are located at two different sites that exhibit two discrete Stern–Volmer constants K_{SV1} and K_{SV2}, respectively. This two-site model accounts for non-linearity commonly observed for Stern–Volmer plots.

In addition to the sensitivity, response times are also important to oxygen sensors. Generally, 95% response time, i.e., $t\downarrow$ (95%, $N_2 \rightarrow O_2$), is defined as the time required for the luminescent intensity to decrease by 95% on changing from 100% nitrogen to 100% oxygen. Similarly, 95% recovery time, i.e., $t\uparrow$ (95%, $O_2 \rightarrow N_2$), means the time required for the luminescent intensity to reach 95% of the initial value recorded under 100% nitrogen on changing from 100% oxygen to 100% nitrogen. Fig. 5 demonstrates the typical dynamic response of the composite materials when switching between fully oxygenated and fully deoxygenated atmospheres. The response times of **1**/MCM-41 (20 mg/g) are about 3 s on going from nitrogen to oxygen ($t\downarrow$) and 26 s on going from oxygen to nitrogen ($t\uparrow$). Especially of **2**/MCM-41 (20 mg/g) are about 2 s ($t\downarrow$) and 29 s ($t\uparrow$), indicating that the emission intensity of the composite materials drops very quickly in the presence of molecular oxygen and have the potential to develop the mesoporous chemical sensors. The obvious difference of the two response times ($t\uparrow$ and $t\downarrow$) can be explained by the stronger adsorption of oxygen than that of nitrogen on mesoporous silica surface [33]. Upon increasing oxygen concentration, the emissive intensity drops very quickly, while upon decreasing oxygen concentration, the emissive intensity increases and recovers to the initial level under 100% nitrogen again. This cycle is repeated in an alternating atmosphere of nitrogen and oxygen, indicating that the emissive intensity changes are reversible. The values of response time ($t\downarrow$), recovery time ($t\uparrow$), and sensitivity are listed in Table 1. Oxygen sensing materials based on **2**/MS show better sensitivity ($I_0/I_1 > 5$) than that based on **1**/MS ($I_0/I_1 > 3$).

4. Conclusions

Novel oxygen sensing materials based on trinuclear starburst Ru(II) complexes assembled in MCM-41 and SBA-15 were prepared. The luminescence of the composite materials exhibits strongly oxygen concentration dependent characteristics and is easily quenched by oxygen. The oxygen sensing properties of **2**/MS is superior to those of **1**/MS. No significant difference is found between

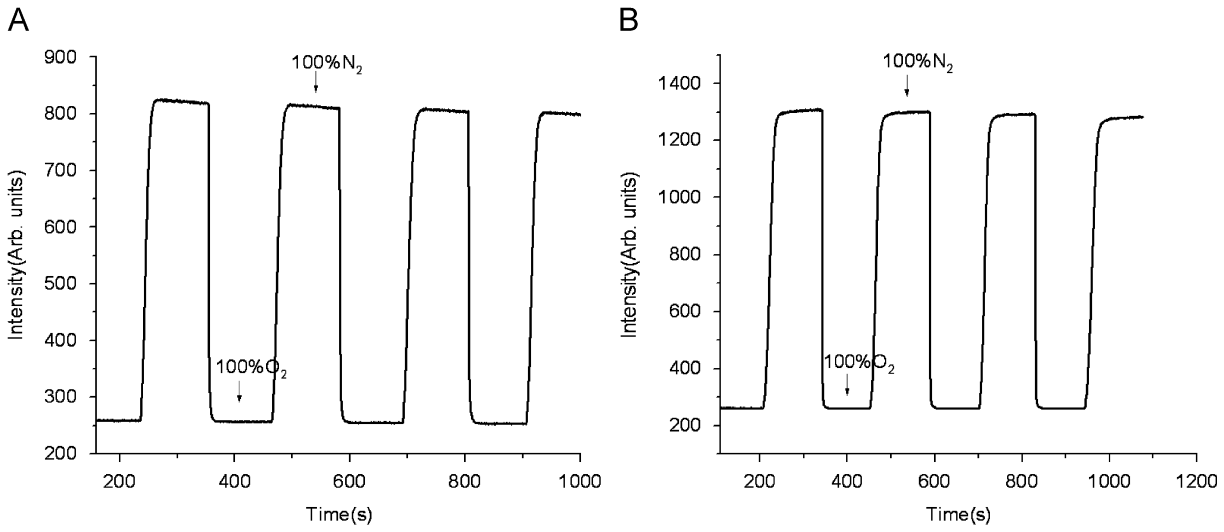

Fig. 5. Response time, relative intensity change, and reproducibility for **1**/MCM-41 (20 mg/g, (A)) and **2**/MCM-41 (20 mg/g, (B)) on switching between 100% nitrogen and 100% oxygen.

Table 1
Oxygen sensing properties of all composite materials

	SBA-15		MCM-41	
	1	**2**	**1**	**2**
I/I_0	3.17	5.39	3.21	5.00
($t\downarrow$) (s)	2.85	2.38	3.32	2.40
($t\uparrow$) (s)	26.6	33.25	25.65	28.50

MCM-41-based and SBA-15-based composite systems. Trinuclear starburst Ru(II) complexes/MS system can be used as oxygen sensors due to their good sensitivity and fast response time.

Acknowledgments

The authors acknowledge the financial supports from One Hundred Talents Project from Chinese Academy of Sciences, the National Natural Science Foundation of China (Projects 20571071).

References

[1] A.K. McEvoy, C.M. McDonagh, B.D. MacCraith, Analyst 121 (1996) 785.
[2] Y. Amao, T. Miyashita, I. Okura, Analyst 125 (2000) 871.
[3] M.A. Chan, S.K. Lam, D. Lo, J. Fluoresc. 12 (2002) 327.
[4] F.G. Gao, A.S. Jeevarajan, M.M. Anderson, Biotechnol. Bioeng. 86 (2004) 425.
[5] C. Huo, H. Zhang, H. Zhang, H. Zhang, B. Yang, P. Zhang, Y. Wang, Inorg. Chem. 45 (2006) 4735.
[6] J.N. Demasa, B.A. DeGraff, Coord. Chem. Rev. 211 (2001) 317.
[7] L. Huynh, Z. Wang, V. Stoeva, A. Lough, I. Manners, M.A. Winnik, Chem. Mater. 17 (2005) 4765.
[8] M.E. Kose, A. Omar, C.a. Virgin, B.F. Carroll, K.S. Schanze, Langmuir 21 (2005) 9110.
[9] B.H. Han, I. Manners, M.A. Winnik, Chem. Mater. 17 (2005) 3160.
[10] M.E. Kose, B.F. Carroll, K.S. Schanze, Langmuir 21 (2005) 9121.
[11] H. Zhang, Y. Sun, K. Ye, P. Zhang, Y. Wang, J. Mater. Chem. 15 (2005) 3181.
[12] R.M. Bukowski, R. Ciriminna, M. Pagliaro, F.V. Bright, Anal. Chem. 77 (2005) 2670.
[13] Y. Tang, E.C. Tehan, Z. Tao, F.V. Bright, Anal. Chem. 75 (2003) 2407.
[14] M.C. DeRosa, P.J. Mosher, G.P.A. Yap, K.S. Focsaneanu, R.J. Crutchley, C.E.B. Evans, Inorg. Chem. 42 (2003) 4864.
[15] M.T. Murtagh, M.R. Shahriari, M. Krihak, Chem. Mater. 10 (1998) 3862.
[16] C. McDonagh, B.D. MacCraith, A.K. McEvoy, Anal. Chem. 70 (1998) 45.
[17] P. Payra, P.K. Dutta, Microporous Mesoporous Mater. 64 (2003) 109.
[18] E. Yavin, L. Weiner, R.A. Yellin, A. Shanzer, J. Phys. Chem. A 108 (2004) 9274.
[19] B. Lei, B. Li, H. Zhang, S. Lu, Z. Zheng, W. Li, Y. Wang, Adv. Funct. Mater. 16 (2006) 1883.
[20] H. Fau, Y. Lu, A. Stump, S.T. Reed, T. Baer, R. Schunk, V. Perezlund, G.P. Lopez, C.J. Brinker, Nature 405 (2000) 56.
[21] G. Wirnsberger, B.J. Scott, G.D. Stucky, Chem. Commun. (2001) 119.
[22] A.B. Descalzo, D. Jimenez, M.D. Marcos, R. Martínez-Máñez, J. Soto, J.E. Haskouri, C. Guillém, D. Beltrán, P. Amorós, M.V. Borrachero, Adv. Mater. 14 (2002) 966.
[23] Y. Ueno, A. Tate, O. Niwa, H.S. Zhou, T. Yamada, I. Honma, Chem. Commun. (2004) 746.
[24] M. Sykora, J.R. Kincaid, P.K. Dutta, N.B. Castagnola, J. Phys. Chem. B 103 (1999) 309.
[25] J.E. Dickeson, L.A. Summers, Aust. J. Chem. 23 (1970) 1023.
[26] E. Amouyal, A. Homis, J. Chem. Soc. Dalton Trans. (1990) 1841.
[27] B. Onida, B. Bonelli, L. Flora, G. Geobaldo, C.O. Arean, E. Garrone, Chem. Commun. (2001) 2216.
[28] D. Zhao, Q. Huo, J. Feng, B.F. Chmelka, G.D. Stucky, J. Am. Chem. Soc. 120 (1998) 6024.
[29] S. Inagaki, S. Guan, Y. Fukushima, T. Ohsuna, O. Terasaki, J. Am. Chem. Soc. 121 (1999) 9611.
[30] G.A. Crosby, J.N. Demas, J. Phys. Chem. 75 (1971) 991.

[31] P. Zhang, J.H. Guo, Y. Wang, W.Q. Pang, Mater. Lett. 53 (2002) 400.
[32] E.R. Carraway, J.N. Demas, B.A. DeGraff, J.R. Bacon, Anal. Chem. 63 (1991) 337.
[33] M.T. Murtagh, M.R. Shahriari, Chem. Mater. 10 (1998) 3862.
[34] J.R. Bacon, J.N. Demas, Anal. Chem. 59 (1987) 2780.
[35] A. Mills, A. Lepre, Anal. Chem. 69 (1997) 4653.
[36] L. Sacksteder, J.N. Demas, B.A. DeGraff, Anal. Chem. 65 (1993) 3480.
[37] A. Yekta, Z. Masoumi, M.A. Winnik, Can. J. Chem. 73 (1995) 202.